Volume 55
Number 6
10 February 2026
Pages 2349-2730

Dalton Transactions

An international journal of inorganic chemistry

rsc.li/dalton

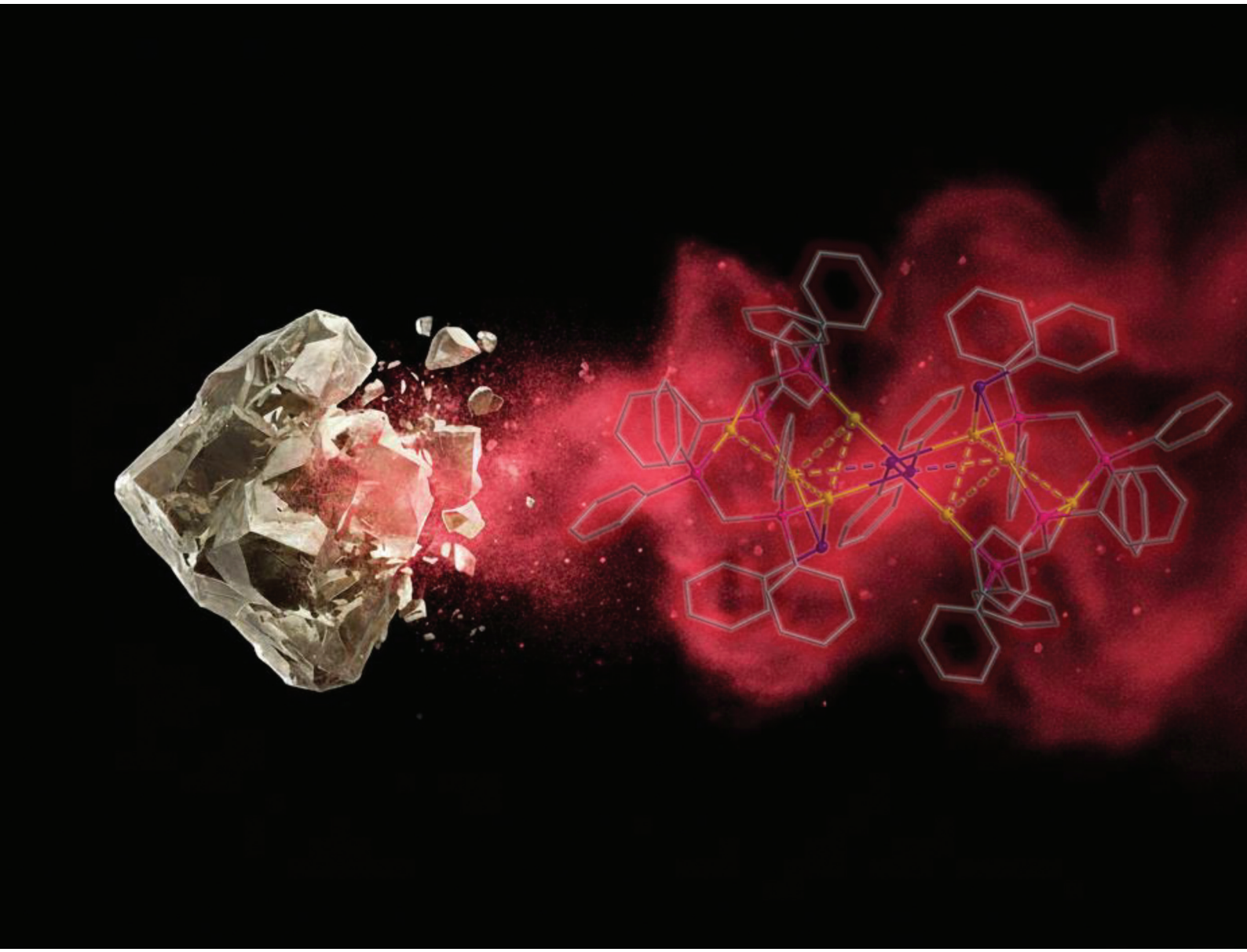

ISSN 1477-9226

ROYAL SOCIETY OF CHEMISTRY

PAPER

Andreas Schnepf *et al.*

$[Au_8(TePh)_4dppm_2(Ph_2PCHPPh_2)_2]Cl_2$: a water and air stable red-luminescent gold–tellurolate cluster with an excellent quantum yield

Dalton Transactions

ROYAL SOCIETY OF CHEMISTRY

PAPER

View Article Online
View Journal | View Issue

Cite this: *Dalton Trans.*, 2026, **55**, 2438

$[Au_8(TePh)_4dppm_2(Ph_2PCHPPh_2)_2]Cl_2$: a water and air stable red-luminescent gold–tellurolate cluster with an excellent quantum yield

Adrian Ott, Wolfgang Leis, Michael Seitz and Andreas Schnepf *

Received 15th October 2025,
Accepted 19th December 2025

DOI: 10.1039/d5dt02489g

rsc.li/dalton

From the reaction of LiTePh and $dppm(AuCl)_2$, a water and air stable gold–tellurolate cluster featuring a novel core structure can be obtained in good yield. The cluster with the formula $[Au_8(TePh)_4dppm_2(Ph_2PCHPPh_2)_2]Cl_2$ **1** exhibits two Au_4 units with Au–Au distances in the range from 295.4 pm to 335.1 pm. Crystals of **1** show red luminescence with a high Stokes shift and an excellent quantum yield (Φ = 0.28), demonstrating that **1** is a promising red phosphor for pc-LED applications.

Introduction

Gold(I) compounds are the focus of extensive research due to their application as, *e.g.*, antirheumatics,[1] catalysts[2] and photoluminescent compounds.[3] Excimer and exciplex formation in gold(I) molecules, preconditioned by aurophilic interactions is thereby one important aspect for the photoluminescence properties.[4] There are numerous gold complexes that exhibit luminescence with excellent quantum yields of up to nearly 100%, but these emit in the high energy spectral range (400–650 nm).[5,6] For gold complexes emitting in the low energy range (>650 nm), which we perceive as red, the quantum yield is significantly lower. This is attributed to the energy gap law.[7–9] In this area, gold(I) chalcogenides are the dominant class of substances.[3,10,11] The most prominent examples are gold–sulphur and more underrepresented gold–selenium compounds.[10–13] Gold–tellurium compounds, on the other hand, have hardly been investigated, although tellurium is one of the few elements with which gold forms minerals in nature, like calaverite ($AuTe_2$), krennerite ($AuTe_2$) and sylvanite ($(Au, Ag)Te_2$).[14–16] Gold–tellurium compounds can be divided into three categories, gold–polytelluride anions,[17–25] gold–tellurides where the Te^{2-} is triply coordinated to three metal atoms,[26–29] and gold–tellurolates, the heavier analogues of thiolates SR, where TeR ligands are present.[30–33] The tellurolate ligand is thereby bound to either one or two metal atoms.[31] A subgroup of these compounds are polynuclear gold–tellurolate clusters, where the core consists of multiple gold and tellurium atoms.[32] Here, only a few examples of such tellurolates are known for gold, in contrast to the other coinage metals, where numerous examples of copper–tellurolate and silver–tellurolate clusters are known.[13] The known gold–tellurolate clusters have the composition $(R_3P)_4Au_8(TeR')_8$ (PR_3 = PPh_3 and PPh_2Py) (R′ = Ph and Tol) and share the same core motif consisting of four gold atoms linearly coordinated by two tellurolates and four gold atoms triply coordinated by two tellurolates and one phosphine ligand (see Fig. 1).[32] To our knowledge, these clusters are also the only gold–tellurolate compounds exhibiting photoluminescence properties.[32]

Results and discussion

In the following, we present the gold–tellurolate cluster $[Au_8(TePh)_4dppm_2(Ph_2PCHPPh_2)_2]Cl_2$ **1** (dppm = bis(diphenyl-

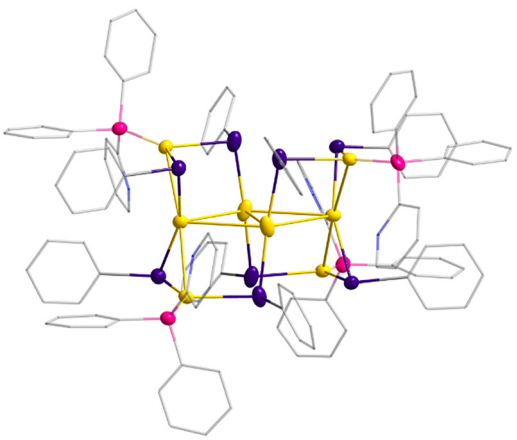

Fig. 1 Molecular structure of $[Au_8(TePh)_8(PPh_2Py)_4]$ in the solid state. Hydrogen atoms and solvent molecules are omitted for clarity. Ph and Py groups are displayed as a wire model. Gold (yellow), tellurium (violet), and phosphorus (pink) atoms are shown as thermal ellipsoids with 50% probability.[32]

Institute of Inorganic Chemistry, University of Tübingen, Auf der Morgenstelle 18, 72076 Tübingen, Germany. E-mail: andreas.schnepf@uni-tuebingen.de

phosphino)methane), which is obtained by the reaction of dppm(AuCl)$_2$ and LiTePh in good yield (64%) as orange crystals. LiTePh is thereby *in situ* prepared from Te_2Ph_2 and L-selectride (LiB[CH(CH$_3$)C$_2$H$_5$]$_3$H). In the ^{31}P-NMR spectrum (in C_6D_6) of the reaction mixture, only one signal at 36.0 ppm is observed. However, from the molecular structure (Fig. 2), it is obvious that four different signals might be expected and thus it is questionable which compound is present in solution prior to crystallization. To clarify this, we performed LR-ESI-MS investigations of the $CHCl_3$ solution used for crystallisation (Fig. S5, SI). A signal at m/z = 1965 is observed, whose isotopic pattern matches the calculated isotopic pattern of the cation $[Au_4(TePh)_2dppm_2]^+$ (Fig. S6, SI). The observation of only one signal in the ^{31}P-NMR spectrum of the reaction solution shows that the phosphine ligands are highly dynamic in solution. Additionally, the missing signal of the doubly charged cation $[Au_8(TePh)_4dppm_2(Ph_2PCHPPh_2)_2]^{2+}$ indicates that the formation of the product takes place during crystallization. This is further supported by the fact that **1** is insoluble in water and in organic solvents. In the solid state ^{31}P-NMR spectrum of **1**, the expected four signals are observed at $\delta(^{31}P)$: 45.2, 37.6, 32.2, and 27.6 ppm (Fig. S3, SI). The two downfield-shifted signals most likely belong to the two phosphorus atoms of the deprotonated dppm ligand. **1** crystallizes in the triclinic space group $P\bar{1}$ and consists of the cationic cluster $[(dppm)_2(Ph_2P(CH)PPh_2)Au_8(TePh)_4]^{2+}$ and two chloride anions that are each coordinated by three chloroform molecules and one of the acidic hydrogen atoms of the dppm ligand. **1** was additionally characterised by ^{13}C-ssMAS-NMR, IR and EDX (Fig. S4, S9, and S11–S14, SI). A detailed structural view of the bonding situation of the halides can be found in the SI (Fig. S1, SI). The core of the centrosymmetric cluster can be described as a dimer of two Au_4Te_2 units (see Fig. 2).

The Au_4Te_2 unit consists of three linearly coordinated Au(I) atoms (Au1, Au3, and Au4) and one triply coordinated Au(I) atom (Au2). These units are brought into close proximity by the dipodal dppm ligands, the tripodal deprotonated dppm ligand and two bridging tellurolate ligands (Table 1). Au1 is linearly coordinated by P11 of the dppm ligand and C213, which is the bridging carbon atom of the deprotonated dppm ligand. The P–Au–C bond angle is 172.6° and the Au1–C213 bond length is 213.6 pm. The phenomenon of dppm ligands undergoing deprotonation to form Au–C bonds is known from the literature.[34] Au3 and Au4 are linearly coordinated, each by the phosphorus atom of the deprotonated dppm ligand and a tellurolate ligand. The bond lengths of Au3–Te1 and Au4–Te2 are 259.8 pm and 258.5 pm, respectively. Au2 is trigonally coordinated by one phosphine and two tellurolates, which is an unusual coordination for gold(I).[35] The Au–Te bond lengths are 273.7 pm (Au2–Te1) and 271.3 pm (Au2–Te2) and thus considerably longer than the Au–Te bonds of the linearly coordinated gold atoms, which might be due to the higher coordination number of the triply coordinated gold atom. The two Au_4Te_2 units in **1** are connected *via* attractive interactions of Au3–Te′2 and Au′3–Te2, which have a distance of 328.8 pm, which is significantly larger than the sum of the single-bond covalent radii of Au (124 pm) and Te (136 pm).[36] Hence, both parts are held together by dispersion forces. Within **1**, a large number of aurophilic interactions are present. The distance of Au1 to the nearest gold atom Au3 is 335.1 pm, which is quite long for an aurophilic interaction. The gold atoms Au2, Au3, and Au4 form a nearly isosceles triangle, with Au3–Au2 and

Table 1 Selected bond lengths [pm] and bond angles [°]

Bond length [pm]		Bond angle [°]	
Au1–Au3	335.08(4)	P21–Au3–Te1	172.05(2)
Au1–C213	213.55(31)	P22–Au4–Te2	166.48(2)
Au1–P11	228.98(9)	P12–Au2–Te1	117.33(2)
Au3–P21	229.14(10)	P12–Au2–Te2	134.55(2)
Au4–P22	227.63(10)	Te1–Au2–Te2	101.022(8)
Au2–P12	229.90(8)		

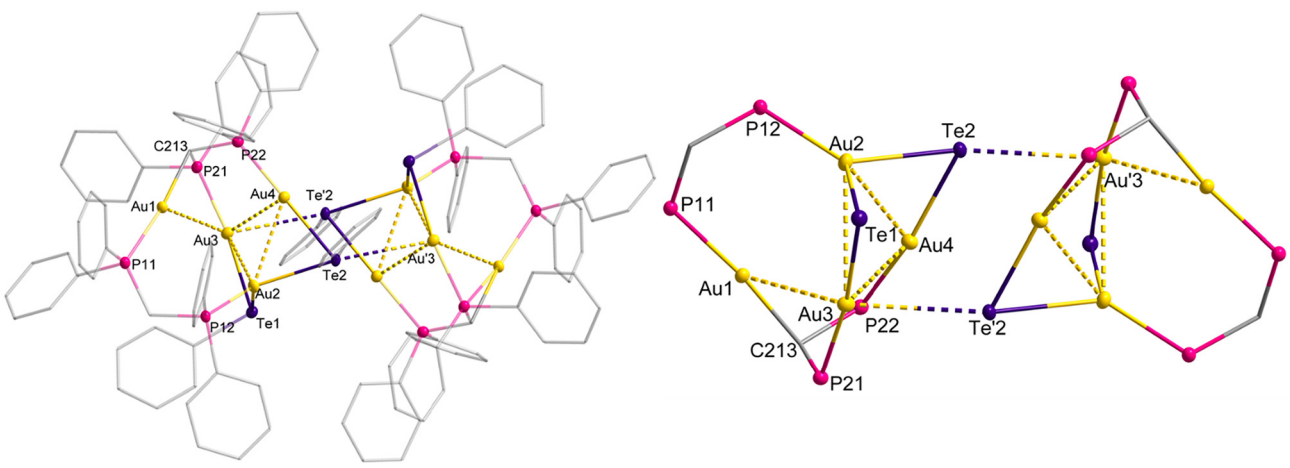

Fig. 2 (Left) Molecular structure of $[Au_8(TePh)_4dppm_2(Ph_2PCHPPh_2)_2]^{2+}$ within **1** in the solid state. Hydrogen atoms, solvent molecules and chlorides are omitted for clarity. Ph groups are displayed as a wire model. (Right) Structure of the core motif: gold (yellow), tellurium (violet), and phosphorus (pink) atoms are shown as thermal ellipsoids with 50% probability. Attractive interactions are shown with dotted lines.

Au3–Au4 atom distances of 326.0 pm and 323.5 pm, respectively. The basis of the triangle Au2–Au4 shows an atom distance of 295.4 pm. Such an isosceles Au_3 triangle motif is also observed within the cluster $Au_8(TePh)_8(PPh_2Py)_4$. There, the Au_3 triangle motifs share the same basis with a short Au–Au distance of 295.2 pm and longer distances of the legs of the triangles of 325.0 pm and 330.1 pm comparable to those of **1**.[32] Also the Au–Te bond lengths in $[Au_8(TePh)_8(PPh_3)_4]$ are similar to those found in **1**. Interestingly, crystals of **1** show bright red luminescence under UV-light as discussed in the following text.

In the solid state, **1** exhibits a broad emission band with a maximum at 715 nm, after excitation at 470 nm. The excitation spectrum shows that the excitation maximum is at 371 nm with emission detection at 685 nm (Fig. 3). The luminescence lifetime in the presence of oxygen, measured at 685 nm, is obtained from a bi-exponential fit, yielding lifetimes of 2.3 μs (46%) and 1.1 μs (54%). The lifetime changes only slightly to 2.2 μs (25%) and 0.9 μs (75%) when switching to an inert argon atmosphere. It cannot be said with certainty whether this is phosphorescence, but the lifetime and Stokes shift suggest that it is, while the fact that oxygen hardly changes the lifetime suggests that it is not. The quantum yield amounts to $\Phi = 0.28$ at room temperature in the solid state in the presence of oxygen. The quantum yield at higher wavelengths is normally lower because of the energy gap law.[8,9] A similar emission maximum of 705 nm is known from the complex [Au(^{Dipp}PZI)(DMAC)] (^{Dipp}PZI = 1,3-bis(2,6-diisopropylphenyl)pyrazinoimidazolium) (DMAC = dimethylacridinide), however, with a lower quantum yield of $\Phi = 0.10$.[7] An example of a thiolate-protected gold cluster is $Au_{24}(SCH_2C_6H_4{}^tBu)_{20}$, which has an emission maximum at 657 nm with a quantum yield of $\Phi = 0.02$.[37] Additionally, a red-emitting heterometallic phosphine-protected ruthenium–gold cluster with an even higher quantum yield of $\Phi = 0.37$ that emits at 720 nm is known. However, in this compound, the photoluminescence is almost completely quenched by O_2.[38] This is not the case for **1**, which shows bright photoluminescence in the presence of oxygen. Consequently, the only gold–tellurolate compounds reported to show photoluminescence are the $(R_3P)_4Au_8(TeR')_8$ clusters and **1**. Both compounds exhibit similar Au_3-triangle motifs with nearly identical bond lengths. However, the emission of **1** is 45 nm red-shifted in comparison with the luminescence of the $[Au_8(TePh)_8(PPh_3)_4]$ cluster in the solid state (λ_{max} = 660 nm).[32]

Additionally, solid **1** is stable up to 153 °C. Beyond this temperature, the cluster decomposes (Fig. S10, SI). **1** can be stored under air for months without decomposition. When crystals of **1** are ground and put under water for two weeks, no decomposition is visible (Fig. 4 (right)). Additionally, the excitation and emission spectra of **1** were recorded before and

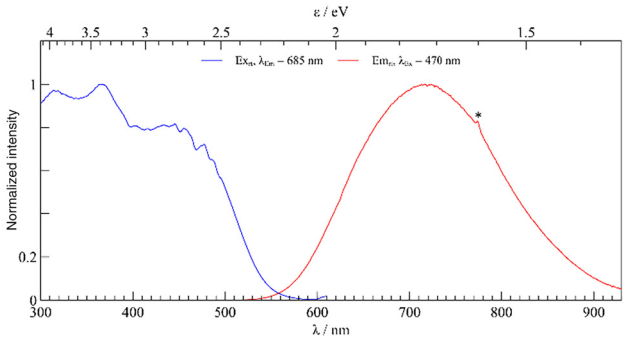

Fig. 3 (Left) Normalized photoluminescence excitation (PLE (blue)) and emission (PL (red)) spectra of **1** in the solid state at room temperature. PLE was recorded with λ(em) = 685 nm and PL with λ(exc) = 470 nm.

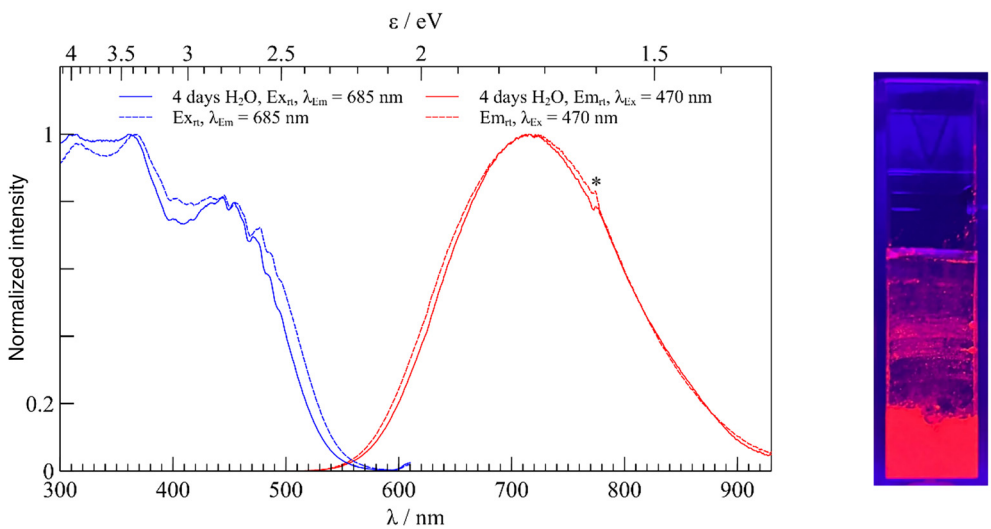

Fig. 4 (Left) Normalized photoluminescence excitation (PLE (blue)) and emission (PL (red)) spectra of **1** in the solid state at room temperature before (dashed) and after 4 days immersed in H_2O (solid). PLE was recorded with λ(em) = 685 nm and PL with λ(exc) = 470 nm. (Right) Cuvette with ground powder of **1** with added water.

after it was immersed for 4 days in water (Fig. 4 (left)). A comparison of the excitation spectra after water immersion shows a small hypsochromic shift. A comparison of the emission spectra reveals a small and seemingly asymmetric change in the band shape, but no significant shift of the maximum. This stability of **1** is atypical for gold tellurium compounds, which usually decompose at room temperature, as evidenced by a precipitation of elemental tellurium. This stability, in addition to the discussed optical properties, demonstrates that **1** is a promising red phosphor for pc-LED applications, since for this high thermal stability and chemical resistance are required (Fig. S15, SI).

Conclusions

We presented the synthesis, structure and luminescence properties of a new gold(I)–tellurolate cluster, with a remarkable stability against water and air. The bright red luminescence at 715 nm, with a quantum yield of Φ = 0.28, combined with the high stability, renders the cluster a promising phosphor for pc-LED applications. It also demonstrates the value of further investigating the underrepresented chemistry and properties of gold(I)–tellurolate clusters. By changing the phosphines and tellurolates, it may be possible to tune the emission wavelength and the solubility and further increase the quantum yield for applications of these compounds in various other fields.

Experimental details

Starting material

The starting materials, Ph_2Te_2 (ref. 39) and dppm$(AuCl)_2$ (ref. 40), were prepared according to the literature. The other chemicals were commercially available.

Preparation of $[(dppm)_2(Ph_2P(CH)PPh_2)Au_8(TePh)_4]Cl_2$ (1)

Ph_2Te_2 (0.205 g, 0.5 mmol) is dissolved in 20 mL of anhydrous THF. 1 M LiB$[CH(CH_3)C_2H_5]_3H$ (L-selectride) in THF (1 mL, 1 mmol) is added and the mixture is stirred for 1 h at room temperature. [dppm$(AuCl)_2$] (0.425 g, 0.5 mmol) is added to the yellow solution and the reaction mixture is stirred for 1 h; afterwards, the solvent is removed in a vacuum. The resulting orange solid is dissolved in 15 mL of chloroform and filtered with a 0.2 μm syringe filter. After a few days, orange crystals are obtained through slow evaporation of the solvent in an open vessel. The remaining chloroform is filtered off and the remaining crystals are washed three times with n-pentane and dried in a vacuum. The product is obtained as orange crystals of **1**. Yield: (396 mg, 0.05 mmol, 64% (yield based on gold)). Analytical data:

^{31}P-CP/MAS-NMR (300 MHz, 6000 Hz): δ [ppm] = 45.2, 37.6, 32.2, 27.6 (Fig. S3, SI).

^{13}C-CP/MAS-NMR (300 MHz, 6000 Hz): δ [ppm] = 138.0, 136.5, 136.0, 134.0, 132.6, 132.1, 131.0, 130.2, 129.8, 128.9, 127.6, 126.5, 112.0, 110.9, 82.4, 32.1 (Fig. S4, SI).

Conflicts of interest

There are no conflicts to declare.

Data availability

Supplementary information (SI): Fig. S2: UV/VIS spectrum of the $CHCl_3$ solution prior to crystallization; Fig. S3 and S4: solid-state NMR data; Fig. S5–S8: mass spectrometric data; Fig. S9: DRIFT spectrum of **1**; Fig. S10: TG/DTA data of **1**; Tables S1 and S2 and Fig. S11–S14: results of SEM and EDX measurements; Table S3: crystallographic parameters of **1**. See DOI: https://doi.org/10.1039/d5dt02489g.

CCDC 2483370 contains the supplementary crystallographic data for this paper.[41]

Acknowledgements

The authors thank Claudio Schrenk for conducting the single-crystal X-ray structure determination, Klaus Eichele for conducting the ssMAS-NMR measurements, Markus Ströbele for conducting the DTA/TG analysis and Elke Nadler for conducting the EDX and REM measurements. We are grateful to the Deutsche Forschungsgemeinschaft (DFG) for financial support.

References

1 J. Aaseth, M. Haugen and Ø. Førre, *Analyst*, 1998, **123**, 3–6.
2 A. S. K. Hashmi and G. J. Hutchings, *Angew. Chem., Int. Ed.*, 2006, **45**, 7896–7936.
3 X. He and V. W.-W. Yam, *Coord. Chem. Rev.*, 2011, **255**, 2111–2123.
4 H. Schmidbaur and H. G. Raubenheimer, *Angew. Chem., Int. Ed.*, 2020, **59**, 14748–14771.
5 M. Baron, C. Tubaro, A. Biffis, M. Basato, C. Graiff, A. Poater, L. Cavallo, N. Armaroli and G. Accorsi, *Inorg. Chem.*, 2012, **51**, 1778–1784.
6 V. R. Naina, S. Gillhuber, C. Ritschel, D. Jin, Shubham, S. Lebedkin, C. Feldmann, F. Weigend, M. M. Kappes and P. W. Roesky, *Angew. Chem., Int. Ed.*, 2025, **64**, e202414517.
7 S. Avula, B. H. Jhun, U. Jo, S. Heo, J. Y. Lee and Y. You, *Adv. Sci.*, 2024, **11**, 2305745.
8 J. A. Treadway, B. Loeb, R. Lopez, P. A. Anderson, F. R. Keene and T. J. Meyer, *Inorg. Chem.*, 1996, **35**, 2242–2246.
9 J. V. Caspar and T. J. Meyer, *J. Phys. Chem.*, 1983, **87**, 952–957.

10 E. R. T. Tiekink and J.-G. Kang, *Coord. Chem. Rev.*, 2009, **253**, 1627–1648.
11 J. M. Forward, D. Bohmann, J. P. Fackler Jr and R. J. Staples, *Inorg. Chem.*, 1995, **34**, 6330–6336.
12 O. Crespo, M. C. Gimeno, A. Laguna, M. Kulcsar and C. Silvestru, *Inorg. Chem.*, 2009, **48**, 4134–4142.
13 O. Fuhr, S. Dehnen and D. Fenske, *Chem. Soc. Rev.*, 2013, **42**, 1871–1906.
14 K. Balzuweit, H. Meekes and P. Bennema, *J. Phys. D: Appl. Phys.*, 1991, **24**, 203.
15 G. Tunell and C. Ksanda, *J. Wash. Acad. Sci.*, 1936, **26**, 507–509.
16 G. Tunell, *Am. Mineral.*, 1941, **26**, 457–477.
17 R. Haushalter, *Inorg. Chim. Acta*, 1985, **102**, L37–L38.
18 R. C. Haushalter, *Angew. Chem., Int. Ed. Engl.*, 1985, **24**, 432–433.
19 S. M. Dibrov and J. A. Ibers, *Commun. Chem.*, 2003, 2158–2159, DOI: 10.1039/B306415H.
20 S. S. Dhingra and R. C. Haushalter, *Inorg. Chem.*, 1994, **33**, 2735–2737.
21 C. Wang and R. C. Haushalter, *Inorg. Chem.*, 1999, **38**, 595–597.
22 S. S. Dhingra, D. K. Seo, G. R. Kowach, R. K. Kremer, J. L. Shreeve-Keyer, R. C. Haushalter and M. H. Whangbo, *Angew. Chem., Int. Ed. Engl.*, 1997, **36**, 1087–1090.
23 D. M. Smith, L. C. Roof, M. A. Ansari, J. M. McConnachie, J. C. Bollinger, M. A. Pell, R. J. Salm and J. A. Ibers, *Inorg. Chem.*, 1996, **35**, 4999–5006.
24 C. J. Warren, D. M. Ho, A. B. Bocarsly and R. C. Haushalter, *J. Am. Chem. Soc.*, 1993, **115**, 6416–6417.
25 M. A. Ansari, J. C. Bollinger and J. A. Ibers, *J. Am. Chem. Soc.*, 1993, **115**, 3838–3839.
26 K. Angermaier and H. Schmidbaur, *Z. Naturforsch. B*, 1996, **51**, 879–882.
27 A. M. Polgar, F. Weigend, A. Zhang, M. J. Stillman and J. F. Corrigan, *J. Am. Chem. Soc.*, 2017, **139**, 14045–14048.
28 J. Olkowska-Oetzel, P. Sevillano, A. Eichhöfer and D. Fenske, *Eur. J. Inorg. Chem.*, 2004, **2004**, 1100–1106.
29 B. J. Frogley, A. F. Hill, C. S. Onn and L. J. Watson, *Angew. Chem., Int. Ed.*, 2019, **58**, 15349–15353.
30 E. S. Lang, C. Maichle-Mössmer and J. Strähle, *Z. Anorg. Allg. Chem.*, 1994, **620**, 1678–1685.
31 P. J. Bonasia, D. E. Gindelberger and J. Arnold, *Inorg. Chem.*, 1993, **32**, 5126–5131.
32 O. Bumbu, C. Ceamanos, O. Crespo, M. C. Gimeno, A. Laguna, C. Silvestru and M. D. Villacampa, *Inorg. Chem.*, 2007, **46**, 11457–11460.
33 N. V. Kirij, W. Tyrra, D. Naumann, Y. L. Yagupolskii, I. Pantenburg and M. Schäfer, *J. Fluor. Chem.*, 2004, **125**, 1933–1938.
34 R. Usón, A. Laguna, M. Laguna, B. R. Manzano, P. G. Jones and G. M. Sheldrick, *J. Chem. Soc., Dalton Trans.*, 1984, 839–843, DOI: 10.1039/DT9840000839.
35 M. C. Gimeno and A. Laguna, *Chem. Rev.*, 1997, **97**, 511–522.
36 P. Pyykkö and M. Atsumi, *Chem. – Eur. J.*, 2009, **15**, 186–197.
37 Z. Gan, Y. Lin, L. Luo, G. Han, W. Liu, Z. Liu, C. Yao, L. Weng, L. Liao, J. Chen, X. Liu, Y. Luo, C. Wang, S. Wie and Z. Wu, *Angew. Chem., Int. Ed.*, 2016, **55**, 11567–11571.
38 S. Takano, H. Hirai, T. Nakashima, T. Iwasa, T. Taketsugu and T. Tsukuda, *J. Am. Chem. Soc.*, 2021, **143**, 10560–10564.
39 J. P. A. Souza, L. R. A. Menezes, F. P. Garcia, D. B. Scariot, P. T. Bandeira, M. B. Bespalhok, S. O. K. Giese, D. L. Hughes, C. V. Nakamura, A. Barison, A. R. M. Oliveira, R. B. Campos and L. Piovan, *Chem. – Eur. J.*, 2021, **27**, 14427–14437.
40 M. J. Harper, E. J. Emmett, J. F. Bower and C. A. Russell, *J. Am. Chem. Soc.*, 2017, **139**, 12386–12389.
41 CCDC 2483370: Experimental Crystal Structure Determination, 2026, DOI: 10.5517/ccdc.csd.cc2pc4qy.